This document was prepared in conjunction with work accomplished under Contract No. DE-AC09-96SR18500 with the U. S. Department of Energy.

DISCLAIMER

Electrochemical Hydrogen Permeability and Oxidation Characteristics of N-Ti-Ni Alloys

J. I. Mickalonis and T. M. Adams
Savannah River National Laboratory
Aiken SC 29803

ABSTRACT

Palladium has been the membrane of choice for hydrogen purification and separation systems because of its high permeability and good mechanical characteristics. Other membrane technologies are being investigated because of the high cost associated with palladium. The Nb-Ti-Ni and V-Ti-Ni alloys were evaluated for their permeability and oxidation characteristics. These alloys have showed some promise in comparison to palladium. Electrochemical testing was conducted in the Devanathan permeation cell and Greene-type electrochemical vessels. The vanadium-based and niobium-based alloys were found to have comparable permeation rates to palladium. The polarization and microstructural characteristics of the alloys were studied to characterize the oxidation and microstructure effects on hydrogen permeation.

Keywords: electrochemical hydrogen permeation, Nb-Ti-Ni alloy, V-Ti-Ni alloy, membranes

INTRODUCTION

Hydrogen separation and purification has been identified as a bottleneck in the development of advanced hydrogen fuel technologies. Many techniques for hydrogen separation are in use or are currently being investigated, such as cryogenic separation, pressure swing adsorption, catalytic purification and selective diffusion. As a result of its high hydrogen permeability, good mechanical characteristics and highly catalytic surface, palladium remains the material of choice in many membrane applications. Palladium and its alloys, however, are costly, making them impractical for large-scale applications. Therefore, an economically feasible, palladium based, commercial scale system would require a significantly reduced amount of palladium or other alloy systems with similar permeation characteristics. Researchers and industry have focused on thin palladium membranes supported on porous substrates and palladium free membranes such as cermets and ceramics for high-pressure, high-temperature applications, as well as the development of new alloys systems.

Palladium and its alloys have been known to possess the ability to dissolve considerable volume of hydrogen and to have increasing permeability with increasing pressure differential

and temperature. However, aside from the high cost palladium also suffers from a low flux and irreversible lattice change during cycling. Palladium coated ceramic membranes offer the potential for extended temperature range operations but suffer from the fatal flaw of 'pinhole" short circuit paths. Any "pinholes" in the palladium-catalytic film on the surface of the ceramic substrate will allow for contaminant/intermediate species to pass directly through the membrane thus effectively reducing the purification factor of the membrane.

Recent efforts in the hydrogen purification and separation membrane have focused on the development and evaluation of non-palladium based membranes that offer a lower cost, high flux, and high durability. Metals from the Group 5A including vanadium, niobium and tantalum are currently being evaluated by various investigators [1-3]. These metals have shown promising results for hydrogen solubility and diffusivity, but suffer from severe hydrogen embrittlement, which makes them unacceptable for membranes. Alloying additions including aluminum, nickel, cobalt, and molybdenum to vanadium have had limited success in decreasing the susceptibility to hydrogen embrittlement [4,5].

The shape memory alloy Ni-Ti also possesses good hydrogen solubility and mechanical properties. The major drawback is that its hydrogen diffusivity is considerably slower than palladium, vanadium, or niobium. Niobium additions to the Ni-Ti alloys have been investigated for their permeation characteristics and mechanical stability [6]. The limited study of these ternary alloys has shown increased permeation (on an order equal to pure palladium) and reasonable mechanical stability in hydrogen. This study attributed the positive results to a duplex microstructure with primary NiTi dendrites surrounded by eutectic of NiTi and NbTi. The dendritic phase was postulated to be the high diffusivity phase while the eutectic structure improved the resistance to hydrogen embrittlement.

In this study, a series of niobium–based alloys and a vanadium–based alloy were investigated for both their electrochemical properties and microstructural characteristics. Palladium was also included as a point of comparison. Testing include cyclic polarization, electrochemical hydrogen permeation and microstructural analysis.

EXPERIMENTAL APPROACH

The alloys were prepared as 25-gram melt buttons using a Centorr System VII arc melter system with a tungsten stinger. Arc melting was performed following evacuation to approximately 10^{-4}Torr then backfilled with argon gas. The V-Ni-Ti Alloys were prepared using 99.7%V, 99.95%Ti, and 99.95% Ni raw materials. The V-Ni-Ti alloy tested as part of this study was of the following alloy composition—51wt%V, 28wt%Ti, and 21wt%Ni. The compositions of the niobium-based alloys were 54wt%Nb, 28wt%Ti, and 18wt%Ni; 51wt%Nb, 28wt%Ti, and 21wt%Ni; 48wt%Nb, 28wt%Ti, and 24wt%Ni. Characterization of the as-cast microstructure was performed using light optical microscopy on ground, polished and etched samples. Scanning electron microscopy and energy dispersive x-ray spectroscopy—including X-ray dot mapping-- were performed to characterize the phase structure and alloying element distribution.

The disk samples for electrochemical testing were sectioned from the arc-melted buttons and prepared via grinding on SiC papers to provide a 600 grit finish. The disk dimensions were approximately 12.5 mm (0.5 in) diameter and 0.64 mm (0.025 in) thick. The hydrogen permeation samples had two wires spot welded near the edge for electrical connections. In

the permeation cell, the exposed surface area was approximately 0.41 cm^2 (0.064 in^2). The samples for electrochemical characterization had a wire attached to one side of the sample with a conductive silver epoxy. The sample was cast into a cylindrical mount with cold-set epoxy. The test surface was ground to a 600 grit finish prior to each test. The exposed surface area was 1.23 cm^2 (0.191in^2). Electrochemical testing was also conducted on palladium foils, which were 99.9% pure. The foils were 0.05 and 0.025 mm 90.002 and 0.001 in) thick.

Hydrogen permeation testing was conducted using a Devanathan and Stachurski type-electrochemical apparatus as shown in Figure 1. The test solution was 0.1M NaOH solution at room temperature. Charging currents were typically 0.1 mA, although values of 0.5 and 1.0 mA were also used. The charging side of the cell was connected to a galvanostat with a floating ground. The applied anodic potential was -0.125 V versus a saturated calomel electrode (SCE), which was housed in a salt bridge containing 0.1M sodium nitrate. Initial experiments were conducted without coating the alloys with a palladium coating. Without the coating no permeations were measured. Subsequent experiments were conducted with both sides of the alloy thinly covered with a plasma-deposited palladium coating.

Testing was conducted following the standard practice ASTM G148-97 [7]. The typical procedure was to bubble nitrogen through the solution for 24 hours in a pre-staging vessel. The solution was gravity fed into the anodic side (anodic potential hold), which had already been de-aerated with nitrogen. The sample was then polarized until a steady background current (10^{-6} to 10^{-7} A/cm^2) was obtained. The de-aerated cathode side (cathodic charging) was then filled with solution and the charging initiated. Nitrogen purging continued throughout the tests.

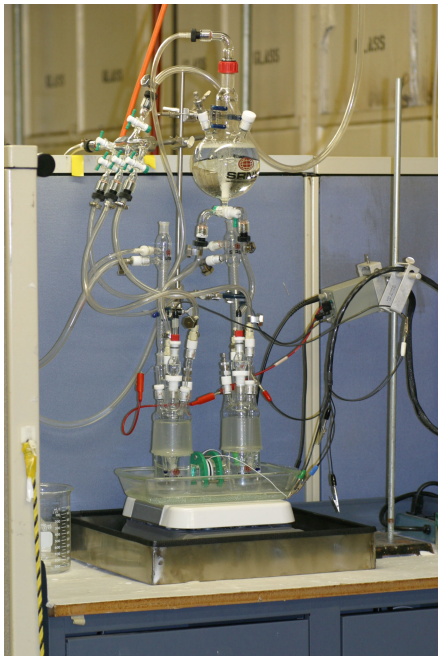

FIGURE 1. Devanathan and Stachurski Electrochemical Hydrogen Permeation Cell

Cyclic potentiodynamic polarization tests (CPP) were conducted on the 48V-28Ti-24Ni alloy and the 54Nb-28Ti-21Ni alloy to characterize the oxidation of the alloys. Testing was

conducted following the standard practice ASTM G61-86 [8]. Tests were conducted in five-port electrochemical vessels. The reference electrode was also a SCE housed in a salt bridge with 0.1M sodium nitrate. The counter electrode was a set of electrically connected graphite rods. Testing was conducted in 0.1M sodium nitrate at room temperature with nitrogen bubbling. The potential was ramped from -300 to 750 mV and back to 0 mV versus the sample open-circuit potential at a rate of 0.5 mV/sec. The potentiostat was under computer control using commercial corrosion software. Prior to performing the CPP, the sample open-circuit potential was allowed to stabilize for twelve hours.

Analysis of the electrochemical permeation data provided a measure of the hydrogen flux through the sample by measuring the steady-state current density I_p (A/cm^2) on the anodic side of the cell. This steady state current density was converted to the steady state hydrogen permeation flux, J_{∞} (mol/m^2s) via equation 1 below.

$$J_{\infty} = I_p/nF \quad (1)$$

The steady-state hydrogen permeation rate, V, (mol/m s), can be defined according to equation 2

$$V = J_{\infty} L = LI_p/nF \quad (2)$$

where L is the sample thickness, I_p is the steady-state current density, n is the number of electrons transferred, and F is Faraday's constant.

RESULTS AND DISCUSSION

The cast alloys solidified dendritically as shown by the photomicrographs in Figure 2 for 48Nb-28Ti-24Ni and 51V-28Ti-21Ni. X-ray mapping of these two alloys, shown in Figure 3, revealed that the dendrites were rich in vanadium for the V-Ni-Ti alloy and in niobium for the Nb-Ni-Ti alloys. The interdendritic areas, which were rich in nickel and titanium, were composed of multiple phases including a ternary eutectic.

Nb48-Ti28-Ni24

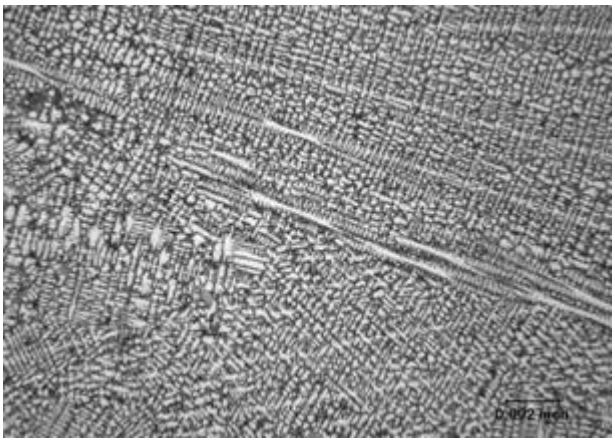

V51-Ti28-Ni21

Figure 2. Photomicrographs of the X-Ni-Ti Alloys

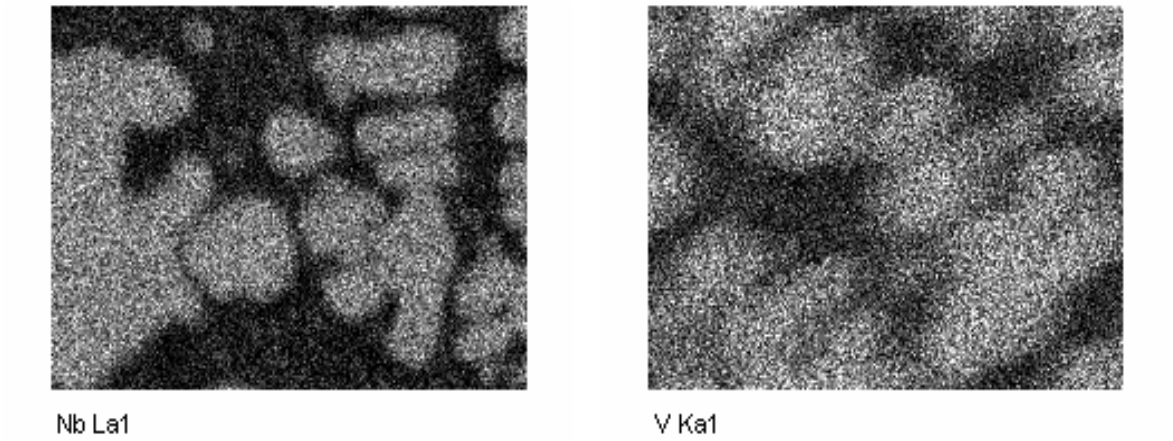

Figure 3. SEM Micrographs and X-ray Mapping of X-Ni-Ti Alloys

The alloys took extended times (> 12 hours) to stabilize to a steady open-circuit potential. The vanadium alloy was more electronegative than the niobium alloy. Average open-circuit potentials were -0.79 V, SCE for V51-Ti28-Ni21 and -0.58 V, SCE for the Nb48-Ti28-Ni24. Palladium had open circuit potentials generally about -0.2 V, SCE. After the potentials were stable, cyclic polarization curves were obtained. Figure 4 show representative curves for each alloy and palladium. The vanadium alloy showed active corrosion with no passive region until reaching a limiting current density of 1 mA/cm^2. The niobium alloy after a small potential range of active corrosion had two different regions of limiting current density, which were presumed to be regions of passivity. Near the corrosion potential the alloys showed similar characteristics. Average Tafel slopes for the two alloys are shown in Table 1.

Table 1. Tafel Slopes for V-Ni-Ti and Nb-Ti-Ni Alloys

	Tafel Slope (mV/decade)	
Alloy	Cathode	Anode
V-Ti-Ni	101	158
Nb-Ti-Ni	174	168

The corrosion current densities for both alloys were approximately 3E-7 A/cm^2, showing the high corrosion resistance of each alloy. This resistance is associated with the material oxide.

The electrochemical hydrogen permeation was performed for a series of niobium alloys (48, 51, 54 wt%), the vanadium alloy and palladium. The oxidizing current chosen for the electrochemical permeation was -0.125 V, SCE. As can be seen in Figure 3, this potential falls within a passive region for both alloys and palladium. Any background current subtraction should then be a constant value. The oxide present on these alloys as noted above also probably contributed to the lack of immediate hydrogen permeability.

Figure 4 shows a plot of oxidizing current versus time for palladium and the vanadium-based alloy at a 0.1 mA/cm^2 charging current. The niobium-based alloys were not plotted since they were near the background current of palladium. This plot clearly demonstrates the greater efficiency of palladium over the alloys.

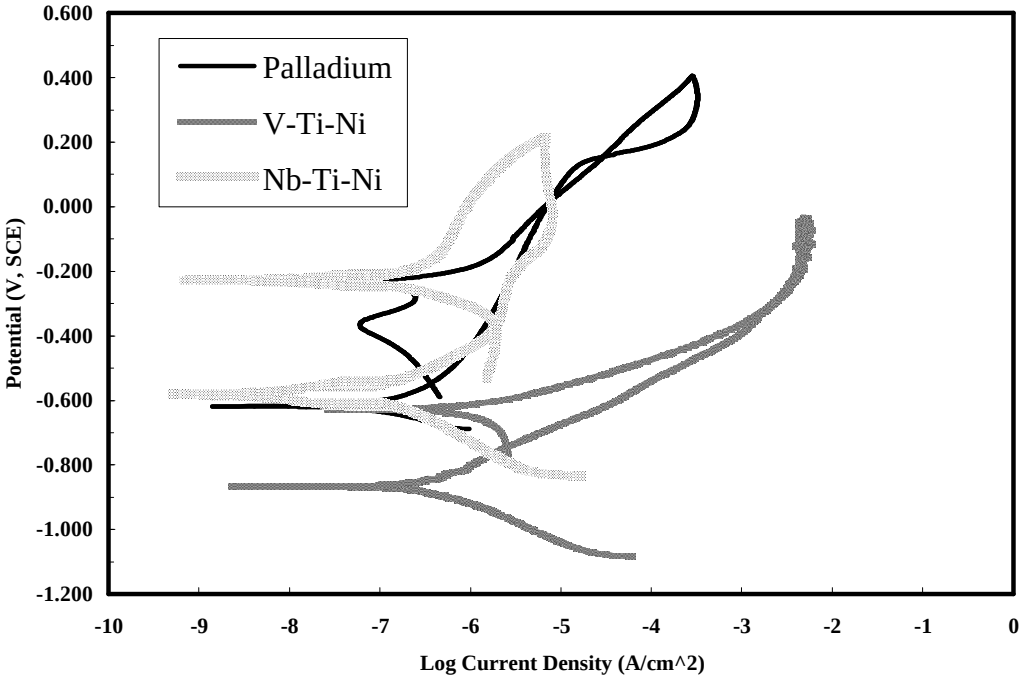

Figure 3. Polarization Curves For Palladium, V-Ti-Ni Alloy and Nb-Ti-Ni alloy

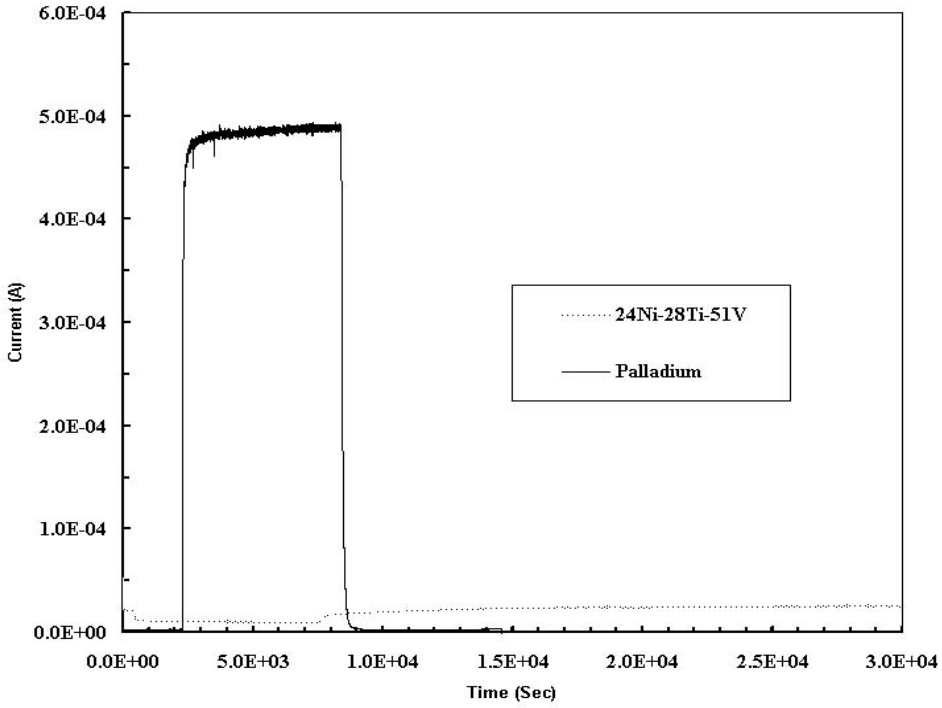

Figure 4. Current Time Scans For Palladium, V-Ti-Ni Alloy and Nb-Ti-Ni Alloys

Each of the alloys reached plateau current values also, but at much lower values as shown in Figure 5, which displays the oxidizing current-time plots for the niobium-based alloys and the vanadium-based alloy. The oxidizing currents increased nearly immediately after the charging

was initiated, similar to palladium. For the niobium alloys, the plateau current values increased with increasing niobium concentration. 51V-28Ti-21Ni, however, had an even greater plateau current than the niobium alloys. The results are summarized in Table 2, listing both the background and oxidizing current for a 0.1 mA/cm^2 charging current.

Table 2. Permeation Values For Palladium, Nb-Ti-Ni and V-Ti-Ni Alloys

Material	Background Current	Oxidizing Current	Permeation Rate
	mA/cm^2	mA/cm^2	mol H_2/m s
Palladium	0.0001	0.082	3.8E-10
48Nb-28Ti-24Ni	0.0013	0.0025	1.2E-10
51Nb-28Ti-21Ni	0.0011	0.0045	2.96E-10
54Nb-28Ti-18Ni	0.0013	0.0057	3.3E-10
51V-28Ti-24Ni	0.015	0.032	2.35E-9

This higher oxidizing current density for palladium translates into a larger steady state hydrogen flux. The permeation rate, however, depends on the sample thickness. For palladium the sample thickness was 0.05 mm, while for the alloys the nominal thickness was 0.635 mm. The overall hydrogen permeation rate as calculated from equation 2 is larger by an order of magnitude for the 51V-28Ti-21Ni alloy as shown in Table 2. For these initial low temperature results the hydrogen permeability of the niobium and vanadium alloys appear to be similar to or better than palladium.

The alloys were also investigated to see if there efficiency (oxidizing current/charging current) was a function of the quantity of hydrogen that was charged. Both the niobium and vanadium alloys showed that as the charging current was increased the efficiency decreased. Figure 6 shows one experiment performed with the 51Nb-28Ti-21Ni for charging current of 0.1, 0.5 and 1.0 mA/cm^2, in which the efficiencies decreased as 40%, 18%, and 12%, respectively. Saturation may be associated with a primary phase that is carrying the hydrogen, but this remains uncertain since all the factors involved with the permeability of these alloys is not currently understood.

Conclusions

As demands become greater for materials that are robust and have good permeation for hydrogen the niobium- and vanadium-based alloys show great promise. From the initial electrochemical characterization the alloys were found to have permeation rates that are comparable to those of palladium. These alloys also showed a decreasing efficiency with increasing current. The microstructures of the alloys were cast with primary dendrites of the 5A elements and eutectic interdendritic phases. The effect of the microstructure on the permeation rates is yet to be studied and understood.

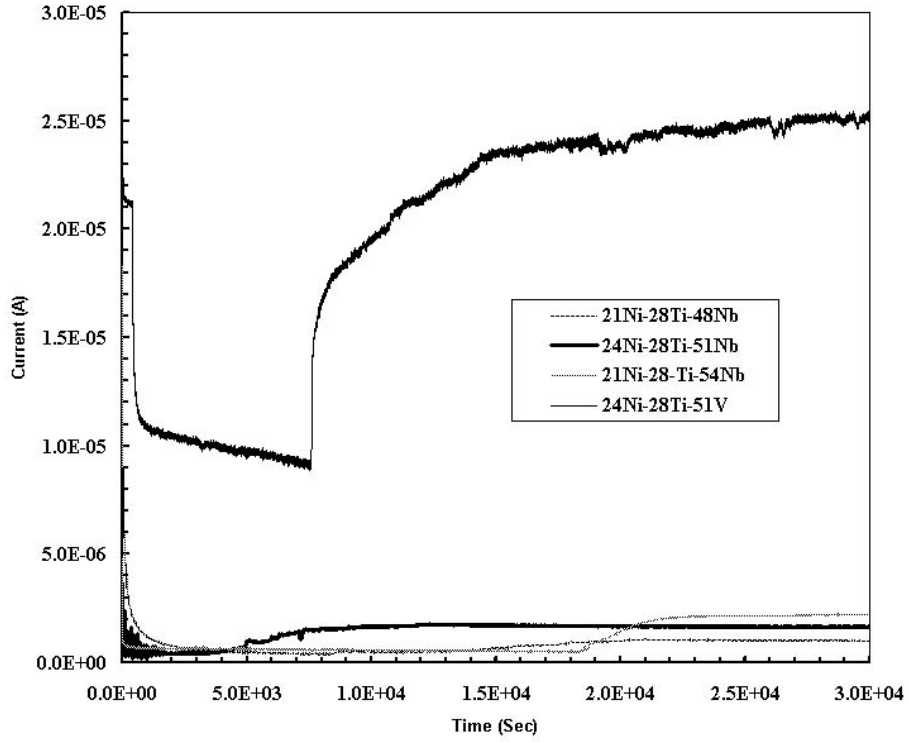

Figure 5. Current Time Scans For Niobium and Vanadium Alloys

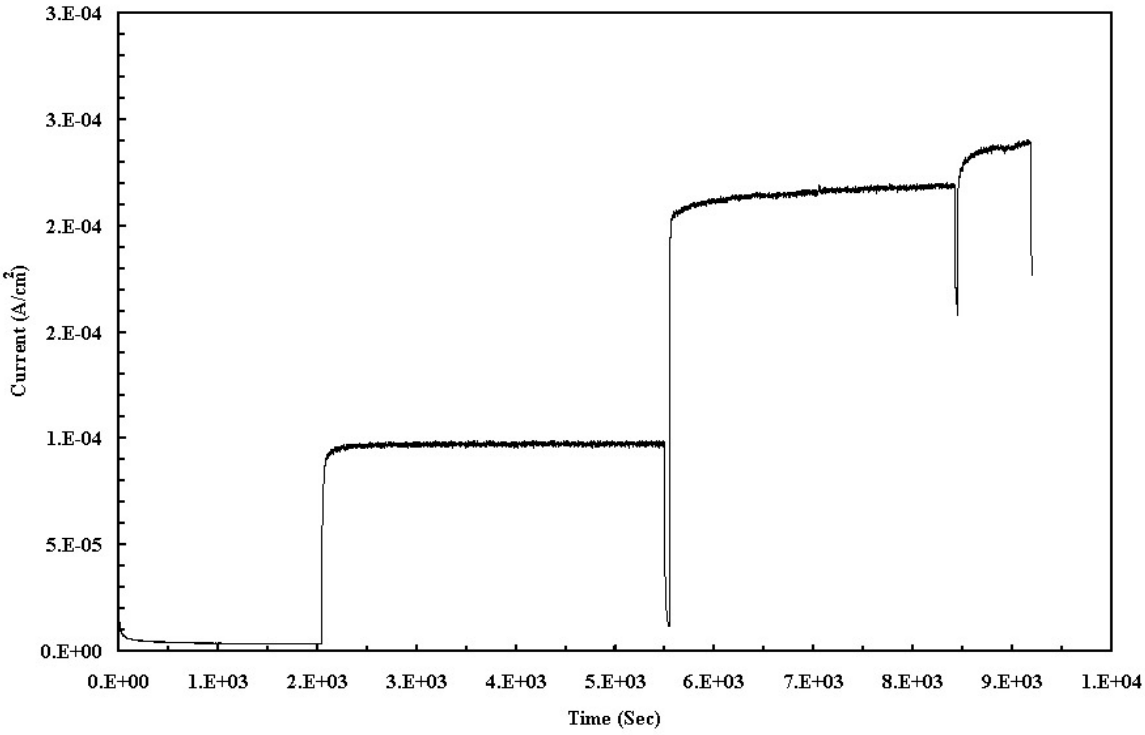

Figure 6. Current Time Scan For 51V-28Ti-21Ni Alloy With Increasing Charging Current

References

1. R. E. Buxbaum and T. L. Marker, Journal of Membrane Science, 85, 29-38, (1993).
2. N. M. Peachey, R. C. Snow, and R. C. Dye, Journal of Membrane Science, 111, 123-133, (1996).
3. T. S. Moss,N. M. Peachey, R. C. Snow, and R. C. Dye, International Journal of Hydrogen Energy, 23, 99-106, (1998).
4. C. Nishimura, M. Komaki, S. Hwang, and M, Amano, Journal of Alloys and Compounds, 330-332, 902-906, (2002).
5. Y. Zhang, T. Ozaki, M. Komaki, and C. Nishimura, Scripta Materialia, 47, 601-606, (2002).
6. K. Hashi, K. Ishikawa, T. Matsuda, and K. Aoki, Journal of Alloys and Compounds, 368, 215-220, (2004).
7. ASTM G148-97, “Uptake of Hydrogen Uptake, Permeation and Transport in Metals by an Electrochemical Technique,” Annual Book of ASTM Standards, ASTM International, West Conshohocken, PA, 2003.
8. ASTM G61-86, “Standard Test Method for Conducting Cyclic Potentiodynamic Polarization Measurements for Localized Corrosion Susceptibility of Iron-, Nickel- or Cobalt-Based Alloys,” Annual Book of ASTM Standards, ASTM International, West Conshohocken, PA, 2003.